

The effect of solution composition on microtubule dynamic instability

Maria J. SCHILSTRA,* Peter M. BAYLEY† and Stephen R. MARTIN

Division of Physical Biochemistry, National Institute for Medical Research, The Ridgeway, Mill Hill, London NW7 1AA, U.K.

The exchange of tubulin dimer into steady-state microtubules was studied over a range of solution conditions, in order to assess the effects of various common buffer components on the dynamic instability of microtubules. In comparison with standard buffer conditions (100 mM-Pipes buffer, pH 6.5, containing 0.1 mM-EGTA, 1.8 mM-MgCl₂ and 1 M-glycerol), the rate and extent of exchange, and thus of dynamic instability, are suppressed by increasing the concentration of glycerol above 2 M. Exchange is enhanced by the addition of further Mg²⁺ (up to 17 mM) or by the addition of Ca²⁺ (up to 0.4 mM). Phosphate ion (150 mM) has relatively little effect on the dynamic behaviour of microtubules, as judged by the exchange method. The findings are interpreted within the framework of the Lateral Cap model for microtubule dynamic instability, in terms of the effects of these changes on the intrinsic rate constants of the system. Changes in the critical concentration are consistent with changes in the absolute values of all dissociation rate constants of the system. By contrast, the extent of tubulin exchange depends selectively on the value of the dissociation rate constant for tubulin-GDP. A decrease in the extent of exchange, and hence in dynamic activity, is associated with a decreased value for this rate constant, and vice versa. The results also show good agreement of predictions of the model in treating the observed variations in the dynamic properties of individual microtubules, induced by different solution conditions.

INTRODUCTION

The property of microtubules that has attracted widespread attention in recent years is that a population of microtubules assembled from tubulin dimer consists of two sub-populations of growing and shrinking microtubules (Mitchison & Kirschner, 1984; Horio & Hotani, 1986; Walker *et al.*, 1988). This property is known as 'dynamic instability'. At steady state of assembly, interconversions between the slowly growing majority state (G-state) and the rapidly shrinking minority state (S-state) occur rather infrequently. The biological implications of this unique phenomenon have been discussed elsewhere (Kirschner & Mitchison, 1986; Sammak & Borisy, 1988; Schulze & Kirschner, 1988; Cassimeris *et al.*, 1988; Kirschner, 1989).

All formulations of microtubule dynamic instability depend on the fundamental observation that tubulin-GDP (Tu-GDP) does not, in general, support microtubule elongation. The species that adds to the end of an elongating microtubule is tubulin-GTP (Tu-GTP); subsequent hydrolysis of GTP produces an unstable core composed of Tu-GDP, which comprises the bulk of the microtubule. It has been assumed that this unstable core is protected by some kind of stable 'cap' generally thought to consist of Tu-GTP. Occasional loss of the 'cap' exposes the unstable Tu-GDP core and the microtubule can enter a shortening phase (G-state→S-state transition) where rapid dissociation of Tu-GDP is observed. The shrinking microtubule is 'rescued' (S-state→G-state transition) when the end is recapped through addition of Tu-GTP [for reviews see Engelborghs (1989) and Bayley (1990) and references cited therein].

The precise temporal relationship between Tu-GTP addition and GTP hydrolysis (which determines the size of the cap) has been controversial. Measurements based on the determination of phosphate production during assembly (Carlier & Pantaloni,

1981; Carlier *et al.*, 1987) suggested that addition and hydrolysis could be uncoupled to such an extent that large Tu-GTP caps [or Tu-GDP-P_i caps (Carlier *et al.*, 1988, 1989)] might exist under certain conditions. Several models for dynamic instability that depend upon the existence of large caps have been described (Hill, 1984; Chen & Hill, 1985*a,b*).

More recent studies (Schilstra *et al.*, 1987; O'Brien *et al.*, 1987, 1990*b*; Voter *et al.*, 1987; Stewart *et al.*, 1990) have been unable to confirm the existence of a substantial Tu-GTP cap. We therefore proposed the Lateral Cap formulation for dynamic instability in which growing microtubules are stabilized by a single layer of Tu-GTP, with GTP hydrolysis effectively coupled to Tu-GTP addition (Bayley & Martin, 1989; Bayley *et al.*, 1988, 1989*a,b,c*, 1990; Bayley, 1990). A recent experimental report by Wilson *et al.* (1990) is consistent with this formalism. This mechanism is further specified by a Hydrolysis Rule, whereby addition of Tu-GTP causes hydrolysis of GTP on a previously terminal Tu-GTP molecule as it becomes incorporated into the microtubule lattice. A growing (G-state) microtubule contains largely Tu-GTP in terminal positions whereas a shrinking (S-state) microtubule has exposed Tu-GDP subunits. In common with other models, the rate constants for the addition and loss of Tu-GTP subunits are assumed to depend upon the precise structure and nucleotide content of the binding site. Detailed evaluation of this model has shown that values of the rate constants determine the overall rates of growth and shrinkage for G-state and S-state microtubules, and strongly influence the lifetimes of the two states and hence the dynamic properties (Bayley *et al.*, 1990). The approach has recently been extended to treat the opposite-end behaviour of dynamic microtubules (Martin *et al.*, 1991).

Numerous experimental studies have shown that the bulk kinetic parameters of microtubule assembly (efficiency of

Abbreviations used: PEM100G, 100 mM-Pipes buffer, pH 6.50, containing 0.1 mM-EGTA, 1.8 mM-MgCl₂ and 1 M-glycerol; PEM100, PEM100G without glycerol; PM100G, PEM100G without EGTA; Tu-GTP, tubulin-GTP; Tu-GDP, tubulin-GDP; C_c, critical concentration (the concentration of free tubulin dimer found at steady state of microtubule assembly); C_p, concentration of polymer; C_t, total concentration of tubulin dimer; C_n, concentration of nucleotide; MAP, microtubule-associated proteins.

* Present address: Department of Bio-organic Chemistry, University of Utrecht, Transitorium 3, Padualaan 8, 3584 CH Utrecht, The Netherlands.

† To whom correspondence should be addressed.

nucleation, critical concentration, rates of assembly and disassembly) are determined by solution conditions. Important variables include metal ion concentration (Martin *et al.*, 1987a; Gal *et al.*, 1988), glycerol concentration (Keates, 1980, 1981; Caplow *et al.*, 1986) and pH and ionic strength (Olmsted & Borisy, 1975; Bayley *et al.*, 1985). Many of these effects probably derive from changes in the intrinsic rate constants for addition and loss of Tu-GTP/Tu-GDP. Thus one might expect that changes in solvent conditions would also have a significant effect on microtubule dynamics through changes in rates of growth/shrinkage and in state lifetimes. Indeed, in some cases such effects have been observed by direct observation of individual microtubules in the optical microscope by enhanced video methods that allow the direct measurement of growing and shrinking state lifetimes and the rates of growth and shrinkage (Walker *et al.*, 1988; O'Brien *et al.*, 1989). However, the addition of many reagents (e.g. Mg^{2+}) will change the critical concentration (C_c) for the system, and the detailed understanding of the effect of such an addition requires a complete re-analysis of the system over a new concentration range.

The incorporation of tubulin into microtubules depends upon the addition of Tu-GTP to the microtubule end; at steady state of assembly this formally resembles an exchange process that can be monitored by uptake of Tu- $[^3H]GDP$. This exchange process is greatly enhanced in the case of dynamic instability. The exchange may be monitored by using a technique that depends upon the non-exchangeability of nucleotide (GDP) bound to polymerized tubulin, plus an efficient enzymic GTP-regenerating system to convert all non-polymer-bound GDP into GTP (Martin *et al.*, 1987b; Schilstra *et al.*, 1987, 1988). The GDP content of the system then gives a direct assay of the microtubule mass. A range of solution conditions can be compared in a single experiment, allowing the critical concentration of the system to be measured and the dynamic properties of the microtubules to be assessed.

In the present investigation the dynamic properties of MAP-free microtubules were examined at steady state under various solution conditions relating to components of buffer systems commonly used for microtubule assembly. We have examined the effects on critical concentration and the kinetics of tubulin exchange into microtubules of buffer ions (phosphate, Pipes), metal ions (Mg^{2+} , Ca^{2+}) and glycerol. These results are used to test the consistency of the Lateral Cap formulation of microtubule dynamics in terms of the effects of changes of individual kinetic constants on dynamic microtubule properties under different solution conditions.

MATERIALS AND METHODS

Materials

GTP, acetate kinase, acetyl phosphate and Pipes (free acid) were from Sigma Chemical Co. $[^3H]GTP$ and $[^{14}C]GTP$ were from Amersham International, and taxol (an anti-tumour agent isolated from *Taxus brevifolia*; Wani *et al.*, 1971) was a gift from Dr. Suffness (National Cancer Institute, National Institutes of Health, Bethesda, MD, U.S.A.). All other chemicals were of the highest grade commercially available and were used without further purification.

Microtubule-associated-protein-(MAP)-free tubulin from bovine brain was prepared as described previously (Clark *et al.*, 1981) by two cycles of assembly and disassembly, followed by phosphocellulose chromatography. Phosphocellulose-purified tubulin was stored in 50 mM-Mes buffer, pH 6.5, containing 0.1 M-EGTA, 7 mM- $MgCl_2$ and 3.4 M-glycerol at $-70^\circ C$. Before the start of each experiment a suitable sample was polymerized and pelleted and the pellet resuspended in an appropriate buffer.

Concentrations of tubulin and taxol were determined by using absorption coefficients of $1.15 \text{ ml} \cdot \text{mg}^{-1} \cdot \text{cm}^{-1}$ at 277 nm for tubulin (Schilstra *et al.*, 1989) and $1.7 \times 10^3 \text{ M}^{-1} \cdot \text{cm}^{-1}$ at 273 nm for taxol (Wani *et al.*, 1971). Taxol was prepared as a 10 mM stock solution in ethanol, and additions to experimental solutions were such that the final ethanol concentration did not exceed 2% (v/v).

All the experiments reported here were carried out in the presence of a GTP-regenerating system (1 unit of acetate kinase/ml and 2.5 mM-acetyl phosphate) without the addition of extra nucleotide, other than the small amounts added as radiolabel.

Determination of critical concentration

In the above protein preparation the total concentration of nucleotide (C_n) in a particular solution (tubulin concentration C_t) is equal to the sum of the exchangeably bound nucleotide plus a small amount of free nucleotide carried through in the pelleting step. Thus each tubulin stock solution was characterized by the factor, a , where:

$$a = C_n/C_t \quad (1)$$

Values of a were determined for all stock solutions used (see below) and were always found to be in the range 1.2–2.

In the presence of the GTP-regenerating system the only GDP present is that contained within the microtubules. Thus the fraction of the total nucleotide present as GDP in a sample of polymerized tubulin is given by $f_{GDP} = C_p/C_n$, where C_p is the concentration of the polymer (in terms of tubulin dimer). Substituting $C_p = C_t - C_c$ (where C_c is the critical concentration) and $C_n = a \cdot C_t$ from eqn. (1) one gets:

$$f_{GDP} = C_p/(a \cdot C_t) = (C_t - C_c)/(a \cdot C_t) \quad (2a)$$

or

$$f_{GDP} \cdot C_t = C_t/a - C_c/a \quad (2b)$$

Therefore a plot of $f_{GDP} \cdot C_t$ against C_t yields $1/a$ as slope and $-C_c/a$ as intercept at $f_{GDP} \cdot C_t = 0$.

Tubulin ($> 50 \mu\text{M}$) plus a small amount of $[^3H]GTP$ was assembled to steady state at $37^\circ C$ in PEM100G buffer plus GTP-regenerating system. Portions of this solution were then diluted to concentrations in the range 2–50 μM , incubated for a further 60 min and then quenched in 2.5% (v/v) $HClO_4$. After neutralization with KOH, the precipitate was spun down, the nucleotides were separated on a Waters Partisil SAX column and the distribution of radioactive label in GMP, GDP and GTP was determined. $f_{GDP(^3H)}$ values were then calculated as radioactivity (c.p.m.) in the GDP peak divided by the sum of the radioactivities (c.p.m.) in the GMP, GDP and GTP peaks (GMP is included because its concentration is typically a few per cent of the total nucleotide concentration, and sometimes it is observed to increase slightly during the experiment). Values of C_c and a were then determined by direct non-linear least-squares fitting to eqn. (2a) by the method of Marquardt (Bevington, 1969).

Determination of polymer mass under different solution conditions

A solution of tubulin ($> 50 \mu\text{M}$) was assembled to steady state at $37^\circ C$ in the presence of GTP-regenerating system and a trace amount of $[^{14}C]GTP$ (or $[^3H]GTP$). The buffer used in this step was PEM100G, except in some studies of the effect of glycerol, where PEM100 was used. This approach circumvents problems associated with different nucleation efficiencies in different buffer systems. Portions of this solution were then adjusted to the desired buffer conditions (addition of glycerol, Ca^{2+} etc.) and incubated for a further 60 min. After precipitation with $HClO_4$, the distribution of label in the different nucleotides was determined as above and $f_{GDP(^{14}C)}$ (or $f_{GDP(^3H)}$) was calculated.

Absolute amounts of non-exchangeable GDP were calculated as follows. Each experiment was designed to include one set of samples in standard PEM100G buffer. As the value of C_c was accurately determined as described above, the value of a could be calculated from eqn. (2a). Thus all other $f_{\text{GDP}^{(14\text{C})}}$ (or $f_{\text{GDP}^{(3\text{H})}}$) values could be converted into concentrations of tubulin dimer present as polymer [e.g., from eqn. (2a), $C_{\text{p}^{(14\text{C})}} = f_{\text{GDP}^{(14\text{C})}} \cdot a \cdot C_t$].

Study of tubulin exchange into microtubules

Tubulin exchange into microtubules at steady state was studied (Martin *et al.*, 1987b) by addition of a small amount of [^3H]GTP (typically $2 \mu\text{M}$; specific radioactivity 400 GBq/mmol) to a solution of microtubules assembled in the appropriate buffer in the presence of [^{14}C]GTP (typically $75 \mu\text{M}$; specific radioactivity 1 GBq/mmol). The exchange was monitored as a function of time, by quenching $20 \mu\text{l}$ samples in HClO_4 at fixed time intervals. Alternatively, exchange as a function of concentration of a buffer component was measured by incubating separate solutions ($30 \mu\text{l}$) for a fixed period of time (typically 60 min) with the second radionucleotide (^3H]GTP) before quenching. The total concentration of polymer is equal to the value of $C_{\text{p}^{(14\text{C})}}$ ($= f_{\text{GDP}^{(14\text{C})}} \cdot a \cdot C_t$). The extent of exchange is assessed as the concentration of polymer labelled with [^3H]GDP ($= C_{\text{p}^{(3\text{H})}} = f_{\text{GDP}^{(3\text{H})}} \cdot a \cdot C_t$). Fractional exchange, F_t , is calculated as the ratio $C_{\text{p}^{(3\text{H})}}/C_{\text{p}^{(14\text{C})}}$ at a given time, t .

RESULTS

Determination of the critical concentration in PEM100G and the effect of taxol

The critical concentration for tubulin dimer in PEM100G was determined as described in the Materials and methods section. Tubulin ($60 \mu\text{M}$) was assembled to steady state at 37°C in the presence of the GTP-regenerating system and a trace amount of [^3H]GTP ($5 \mu\text{M}$; specific radioactivity 400 GBq/mmol). Portions of this solution were then diluted to final tubulin concentrations

(C_t) in the range $2\text{--}59 \mu\text{M}$. In order to check the validity of the approach, parallel samples for four different final C_t values were diluted into an excess of taxol ($120 \mu\text{M}$ -taxol for $C_t = 49 \mu\text{M}$ and $50 \mu\text{M}$ -taxol for $C_t = 5, 11$ and $27 \mu\text{M}$). The solutions were then equilibrated for a further 60 min at 37°C and values of $f_{\text{GDP}^{(3\text{H})}}$ were calculated as described above. Non-linear least-squares analysis of 37 data points according to eqn. (2a) gave $a = 1.38 \pm 0.01$ and $C_c = 4.1 \pm 0.5 \mu\text{M}$. The results of this experiment are presented as a linear plot in Fig. 1(a). The four concentration values for tubulin plus taxol gave the same slope within experimental error, as expected. An accurate value for the C_c in the standard buffer is important, since it is used in the calculation of a and hence in the conversion of f_{GDP} values into absolute GDP concentrations.

A separate determination of the C_c value in the presence of taxol was made by using a similar approach. Tubulin dimer solutions containing taxol, GTP-regenerating system and a trace of [^3H]GTP were prepared at a series of protein concentrations in the range $1\text{--}70 \mu\text{M}$. The amount of taxol used in each solution was sufficient to saturate at least 98% of the tubulin, calculated by using a K_d value of $0.87 \mu\text{M}$ (Parness & Horwitz, 1981). These solutions were then polymerized by incubating for 60 min at 37°C and values of $f_{\text{GDP}^{(3\text{H})}}$ were determined as described above. Analysis of the data (33 points) according to eqn. (2a) gave $a = 1.454 \pm 0.004$ and $C_c = 0.80 \pm 0.2 \mu\text{M}$ (Fig. 1b). This experiment also confirms that microtubules formed in the presence of taxol do hydrolyse GTP and that the resulting microtubule-bound GDP is non-exchangeable.

Effects of glycerol on the critical concentration and tubulin exchange kinetics

The effects of glycerol on the C_c and on tubulin exchange kinetics in PEM100 buffer were studied by polymerizing tubulin ($60 \mu\text{M}$) in PEM100 in the presence of [^{14}C]GTP and the GTP-regenerating system. After steady state had been reached (60 min), the solution was divided into $25 \mu\text{l}$ portions and equilibrated for a further 60 min at 37°C with $25 \mu\text{l}$ of PEM100 containing different concentrations of glycerol (final [glycerol] = $0\text{--}3.5 \text{ M}$, final $C_t = 30 \mu\text{M}$). Then $2 \mu\text{M}$ -[^3H]GTP was added (specific radioactivity 400 GBq/mmol), and the solutions were incubated for a further 60 min at 37°C before being quenched with HClO_4 .

The total polymer concentration ($= C_{\text{p}^{(14\text{C})}}$; see above) under the standard conditions (1 M -glycerol) is $25.9 \mu\text{M}$ ($C_t = 30 \mu\text{M}$, $C_c = 4.1 \mu\text{M}$). Fig. 2(a) shows that the C_c ranges from $8(\pm 1.5) \mu\text{M}$ in the absence of glycerol to less than $1 \mu\text{M}$ at [glycerol] $> 2.5 \text{ M}$. Fig. 2(a) also shows that the incorporation of tubulin into microtubules in 60 min at 37°C is strongly suppressed by increasing glycerol concentrations. Fractional exchange into steady-state microtubules in 60 min, F_{60} ($= C_{\text{p}^{(3\text{H})}}/C_{\text{p}^{(14\text{C})}}$), is shown in Fig. 2(b). F_{60} is $0.43(\pm 0.05)$ under standard conditions (1 M -glycerol); in the absence of glycerol F_{60} is increased to $0.62(\pm 0.07)$, whereas at high glycerol concentrations ($> 2.5 \text{ M}$) it decreases to approx. 0.1.

Effects of Ca^{2+} and Mg^{2+} on critical concentration and tubulin exchange kinetics

The effects of CaCl_2 and MgCl_2 on the critical concentration of tubulin dimer in a buffer system containing 100 mM -Pipes and 1 M -glycerol was studied. Two samples of tubulin ($30 \mu\text{M}$) were polymerized at 37°C for 60 min in the presence of [^3H]GTP and the GTP-regenerating system. The buffer was PEM100G for studies of the effect of Mg^{2+} and was PM100G for studies of the effect of Ca^{2+} . After incubation, each sample was divided into several portions and Mg^{2+} (or Ca^{2+}) was added to the desired final concentration. These portions ($C_t = 23 \mu\text{M}$) were then

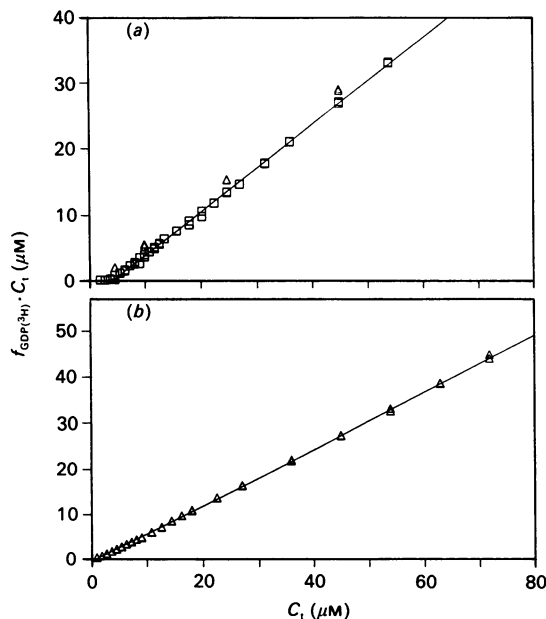


Fig. 1. Determination of critical concentration

Plot of $f_{\text{GDP}^{(3\text{H})}} \cdot C_t$ against tubulin concentration (C_t) for: (a) tubulin dimer in PEM100G buffer (\square) and taxol control experiments (\triangle); (b) tubulin dimer plus taxol in PEM100G buffer. The slope is $1/a$ and the intercept at $f_{\text{GDP}^{(3\text{H})}} \cdot C_t = 0$ is $-C_c/a$ (see the text).

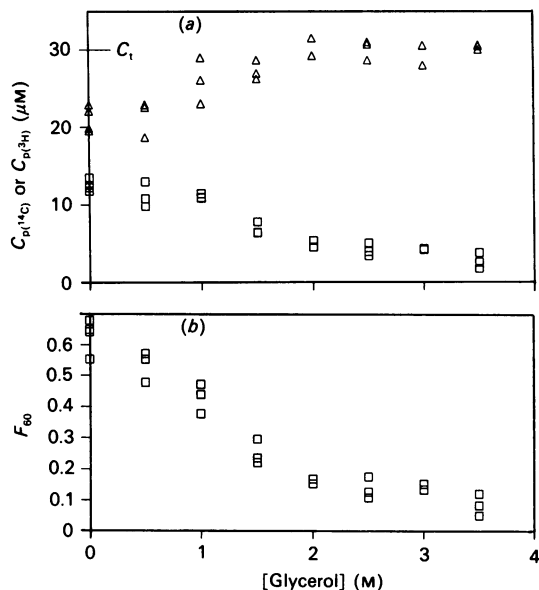


Fig. 2. Effect of glycerol on the critical concentration of tubulin exchange

(a) Total polymer mass (measured as $C_{p(^{14}C)}$; Δ) and extent of exchange after 60 min (measured as $C_{p(^3H)}$; \square) as a function of [glycerol]. $C_t = 30 \mu\text{M}$. (b) Fractional exchange at 60 min, F_{60} ($= C_{p(^3H)}/C_{p(^{14}C)}$), as a function of [glycerol] (data from part a).

incubated for a further 30 min before being quenched with HClO_4 . Fig. 3 shows that, even though both metal ions decrease the steady-state polymer mass (i.e. they increase the C_c), they are effective in very different concentration ranges. Thus, whereas 1 mM- Ca^{2+} increases the C_c from 4.1 μM to approx. 19 μM , the effect of Mg^{2+} is much smaller, 10 mM- Mg^{2+} only increasing the C_c to approx. 8.0 μM .

The effects of metal ions on the exchange of tubulin into microtubules were studied by polymerizing tubulin in the presence of the GTP-regenerating system and 80 μM - $[^{14}\text{C}]\text{GTP}$ (specific radioactivity 0.8 GBq/mmol) in either PEM100G (Mg^{2+} experiment) or PM100G plus 0.05 mM-EGTA (Ca^{2+} experiment). After polymerizing for 30 min, the solutions were divided into two parts. One half was equilibrated with MgCl_2 (15 mM) or CaCl_2 (0.4 mM) and the other half served as a control (final $C_t = 23 \mu\text{M}$ for all samples). Then 1.5 μM - $[^3\text{H}]\text{GTP}$ (specific radioactivity 400 GBq/mmol) was added to each of the samples and portions from these samples were quenched with HClO_4 at various times over a period of approx. 2 h.

The calculated polymer concentration in the controls was 18.9 μM ($C_t = 23 \mu\text{M}$, $C_c = 4.1 \mu\text{M}$; see above). In the presence of added metal ions the observed steady-state polymer concentrations were decreased to $9.1 \pm 0.6 \mu\text{M}$ (0.4 mM- Ca^{2+}) and $16 \pm 1.0 \mu\text{M}$ (15 mM- Mg^{2+}) (see Fig. 3). The increase of fractional exchange ($F_t = C_{p(^3H)}/C_{p(^{14}C)}$) as a function of time is presented in Figs. 4(a) and 5(a). It is clear that increasing either the Ca^{2+} or the Mg^{2+} concentration in these experiments leads to a significant increase in the rate and extent of the exchange processes compared with the controls.

In order to assess the effects of different concentrations of these metal ions on the exchange process, tubulin (60 μM) was assembled in PEM100G (Mg^{2+} experiment) or PM100G (Ca^{2+} experiment) in the presence of $[^{14}\text{C}]\text{GTP}$ and the GTP-regenerating system. After steady state had been reached, the solutions were divided into 25 μl portions and equilibrated for a further 60 min at 37 $^\circ\text{C}$ with 25 μl of PEM100G (Mg^{2+} experiment) or PM100G (Ca^{2+} experiment) containing different concentrations of MgCl_2 or CaCl_2 as appropriate. Then 0.5 μM -

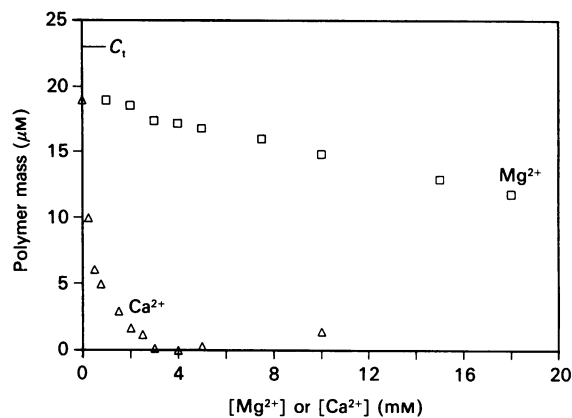


Fig. 3. Effects of Mg^{2+} and Ca^{2+} on the critical concentration in PEM100 buffer

Total polymer mass (measured as $C_{p(^3H)}$) plotted as a function of [Mg^{2+}] (\square) and [Ca^{2+}] (Δ). $C_t = 23 \mu\text{M}$; C_c (PEM100) = 4.1 μM .

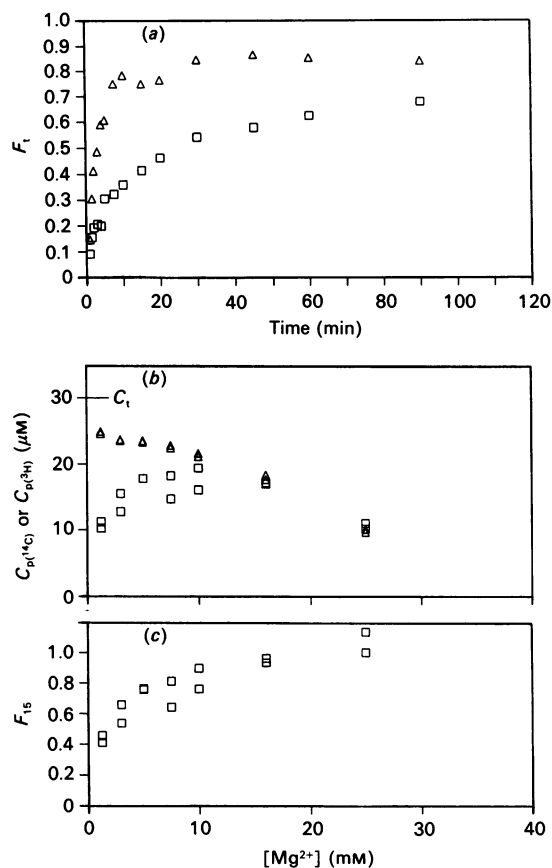


Fig. 4. Effect of Mg^{2+} on tubulin exchange

(a) Fractional exchange, F_t ($= C_{p(^3H)}/C_{p(^{14}C)}$) as a function of time for PEM100G plus 15 mM- Mg^{2+} (Δ) compared with the control experiment in PEM100G (\square). (b) Total polymer mass (measured as $C_{p(^{14}C)}$; Δ) and extent of exchange after 15 min (measured as $C_{p(^3H)}$; \square) as a function of [Mg^{2+}]. $C_t = 30 \mu\text{M}$. (c) Fractional exchange at 15 min, F_{15} ($= C_{p(^3H)}/C_{p(^{14}C)}$), as a function of [Mg^{2+}] (data from part b).

$[^3\text{H}]\text{GTP}$ (specific radioactivity 400 GBq/mmol) was added, and the solutions were incubated for a further 15 min at 37 $^\circ\text{C}$ before being quenched with HClO_4 . The results are shown in Figs. 4(b) and 5(b). Fig. 4(b) shows the values of $C_{p(^3H)}$ (extent of exchange) and $C_{p(^{14}C)}$ (total polymer mass) as a function of [Mg^{2+}]. This

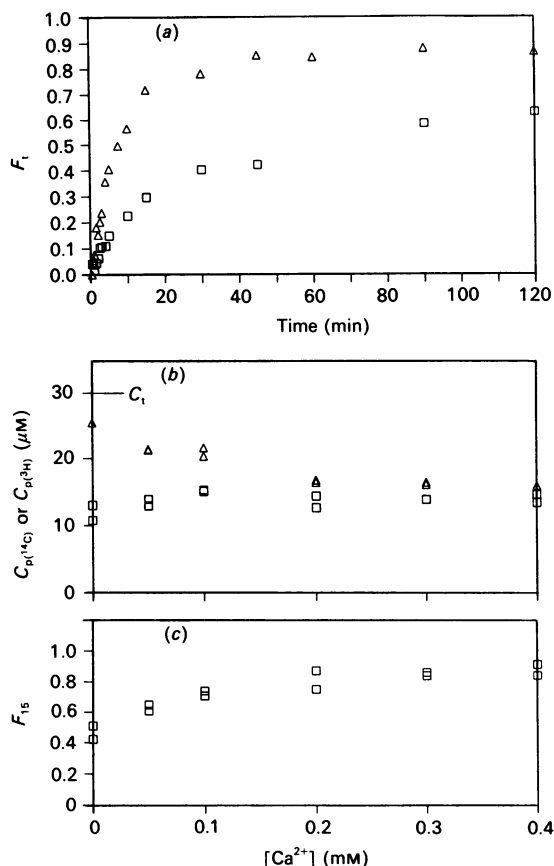


Fig. 5. Effect of Ca^{2+} on tubulin exchange

(a) Fractional exchange, F_t ($= C_{p(3H)}/C_{p(14C)}$) as a function of time for PM100G plus 0.4 mM- Ca^{2+} (Δ) compared with the control experiment in PM100G (\square). (b) Total polymer mass (measured as $C_{p(14C)}$; Δ) and extent of exchange after 15 min (measured as $C_{p(3H)}$; \square) as a function of $[\text{Ca}^{2+}]$. $C_t = 30 \mu\text{M}$. (c) Fractional exchange at 15 min, F_{15} ($= C_{p(3H)}/C_{p(14C)}$), as a function of $[\text{Ca}^{2+}]$ (data from part b).

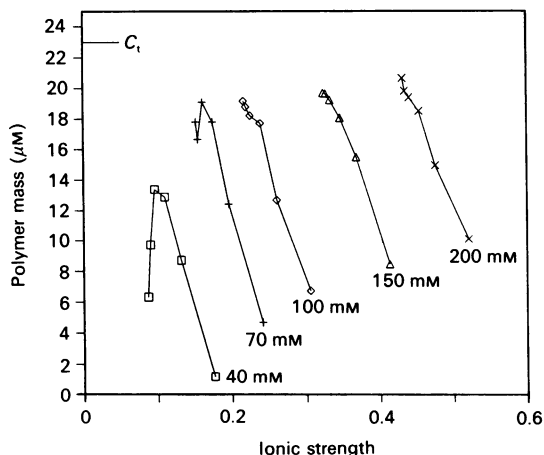


Fig. 6. Effect of Mg^{2+} on the critical concentration at different Pipes concentrations

Total polymer mass (measured as $C_{p(3H)}$) plotted as a function of $[\text{Mg}^{2+}]$ for 40 mM- (\square), 70 mM- (+), 100 mM- (\diamond), 150 mM- (Δ) and 200 mM-Pipes (\times). Each of the five curves shows (left to right) data for 0.2 mM-, 1.2 mM-, 3.2 mM-, 7.7 mM-, 15 mM- and 30 mM- Mg^{2+} . Values of [Pipes] are indicated in the Figure. $C_t = 23 \mu\text{M}$; C_c (PEM100G) = 4.1 μM .

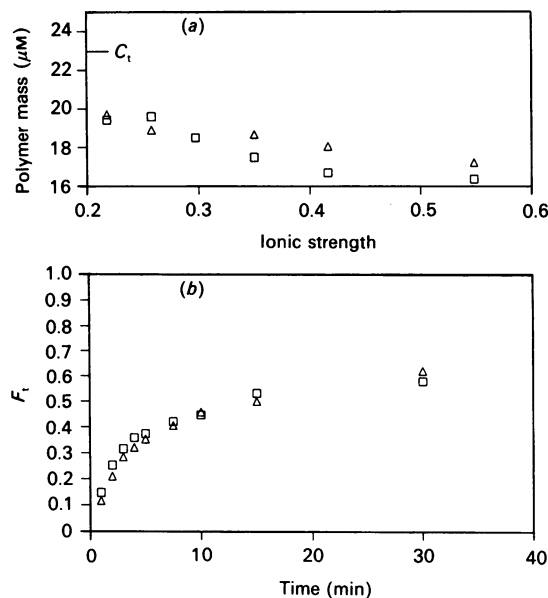


Fig. 7. Effect of sodium phosphate and NaCl on critical concentration and tubulin exchange in PEM100 buffer

(a) Total polymer mass (measured as $C_{p(3H)}$) plotted as a function of ionic strength for sodium phosphate (\square) and NaCl (Δ). $C_t = 23 \mu\text{M}$; C_c (PEM100G) = 4.1 μM . (b) Fractional exchange, F_t ($= C_{p(3H)}/C_{p(14C)}$) as a function of time for PEM100G plus 150 mM-sodium phosphate (\square) compared with PEM100G plus 200 mM-NaCl (Δ).

result shows that the C_c value falls as $[\text{Mg}^{2+}]$ increases (cf. Fig. 3) and that the absolute amount of exchange first rises and then falls as $[\text{Mg}^{2+}]$ increases. Very similar results are shown in Fig. 5(b) for Ca^{2+} but at much lower concentration (0–0.4 mM). The fractional exchange after 15 min, F_{15} ($= C_{p(3H)}/C_{p(14C)}$) under standard conditions (PEM100G) is 0.4. Upon increasing either $[\text{Mg}^{2+}]$ or $[\text{Ca}^{2+}]$ the F_{15} value increases and becomes greater than 0.9 for $[\text{Mg}^{2+}]$ greater than 12 mM or for $[\text{Ca}^{2+}]$ greater than 0.2 mM (Figs 4c and 5c).

Influence of Pipes buffer on the effect of Mg^{2+} on the critical concentration

In order to study the possible influence of the buffer itself experiments from the previous section were repeated with different concentrations of Pipes. Tubulin (60 μM) was assembled to steady state in PEM100G in the presence of $[\text{3H}]\text{GTP}$ and the GTP-regenerating system, and then diluted with an appropriate buffer to give a final C_t of 23 μM in final [Pipes] varying from 40 to 200 mM and final $[\text{Mg}^{2+}]$ ranging from 0.2 to 30 mM. After equilibration (30 min at 37 $^{\circ}\text{C}$), the protein was precipitated and the nucleotide composition was analysed. The results are presented in Fig. 6, which shows the amount of polymer formed ($= C_{p(3H)}$) for different concentrations of Mg^{2+} and Pipes.

At high concentrations of Pipes (> 80 mM) the greatest amount of polymer is formed at low values of $[\text{Mg}^{2+}]$ (0.2–1.7 mM). Increasing $[\text{Mg}^{2+}]$ beyond this range decreases the polymer mass (cf. Fig. 3). For a particular $[\text{Mg}^{2+}]$, the amount of polymer formed increases as the concentration of Pipes increases. At low concentrations of Pipes (< 80 mM) somewhat different behaviour is observed. As $[\text{Mg}^{2+}]$ is increased the amount of polymer formed first rises and then falls. At the lowest Pipes concentration studied (40 mM) the amount of polymer formed at the optimum $[\text{Mg}^{2+}]$ is only 71 % of that formed in the control. These results show that optimal assembly is a function of both Pipes and Mg^{2+} , and that factors other than ionic strength are important.

Effects of phosphate on C_c and the microtubule dynamics

The effect of phosphate ion on the critical concentration of tubulin dimer in a buffer containing 100 mM-Pipes and 1 M-glycerol was studied as follows. Tubulin (30 μM) was polymerized at 37 °C (60 min) with [^3H]GTP and the GTP-regenerating system. The sample was then divided into several portions and sodium phosphate (or NaCl as control) was added to the desired final concentration. These portions ($C_c = 23 \mu\text{M}$) were incubated for a further 30 min and then quenched with HClO_4 . Fig. 7(a) shows that the effect of increasing ionic strength is small and effectively the same for sodium phosphate and NaCl (and for sodium acetate and Na_2SO_4 ; results not shown); the C_c increases from 3.5 μM (23–19.5) at $I 0.2$ to approx. 6 μM at $I 0.56$.

The effect of phosphate on the exchange of tubulin into microtubules was studied as follows. Tubulin was polymerized in PEM100G in the presence of GTP-regenerating system and 80 μM -[^{14}C]GTP (specific radioactivity 0.8 GBq/mol). This solution was then split into two parts. One part was equilibrated with 150 mM-sodium phosphate and the other with 200 mM-NaCl. Then 1.5 μM -[^3H]GTP (specific radioactivity 400 GBq/mmol) was added to each sample and portions were quenched with HClO_4 at various times over a 30 min period. The two samples showed nearly identical behaviour (see Fig. 7b); in both cases a substantial degree of exchange is evident over a 40 min period, indicating dynamic activity of the same degree as under the standard conditions in PEM100G.

DISCUSSION

We have studied the effects of changes in various solution conditions on the C_c and the tubulin exchange behaviour of microtubules prepared from MAP-free tubulin.

The method used here in the determination of the C_c uses small amounts of material per measurement (approx. 60 μg) and, unlike other methods, is accurate for data points obtained at C_c values close to the C_c . Furthermore, this approach obviates problems associated with relating turbidity to polymer mass and the problems of quantitative separation of polymer and monomer in centrifugation procedures. The microtubules formed in our standard buffer system (PEM100G) appear to be almost entirely of normal morphology; very few aberrant structures are formed (Karecla *et al.*, 1989). The data reported here for other buffer conditions were obtained with microtubules originally prepared in this standard buffer. The formation of a small proportion of aberrant structures under extreme conditions cannot be excluded and could be responsible for the presence of some residual non-exchangeable GDP.

Repeated measurements of the C_c in the standard buffer gave a value of $4.1 \pm 0.5 \mu\text{M}$. This value is important for two reasons. First, it is used in the calculation of a for any tubulin preparation and hence in the conversion of f_{GDP} values into amounts of labelled tubulin dimer present as polymer. Secondly, the C_c values under different buffer conditions are derived directly from this value (see the Results section).

Effects of solution conditions on the microtubule critical concentration

Decreasing [glycerol] to zero increases the C_c to $8 \pm 1.5 \mu\text{M}$; increasing [glycerol] lowers the C_c to less than 1 μM for concentrations of glycerol greater than 2.5 M. The ability of Ca^{2+} and Mg^{2+} to inhibit microtubule formation and to induce disassembly of pre-formed microtubules has been known for many years (e.g. see Olmsted & Borisy, 1975). For MAP-containing microtubules we have shown (Gal *et al.*, 1988) that 50% disassembly of pre-formed microtubules (in a Mes-containing buffer at 25 °C) can be induced by approx. 0.6 mM- Ca^{2+}

or by approx. 3 mM- Mg^{2+} (cf. Olmsted & Borisy, 1975). For the tubulin dimer microtubules studied here we find that the effect of Ca^{2+} is very similar (50% disassembly at 0.4 mM- Ca^{2+} ; Fig. 3). However, Mg^{2+} appears to be much less effective in disassembling pre-formed dimer microtubules; 50% disassembly is only found at [Mg^{2+}] > 15 mM and complete disassembly requires [Mg^{2+}] \geq 30 mM, depending upon the ionic strength.

Three other findings relating to changes C_c are of interest. First, the effect of increasing the ionic strength on the stability of pre-formed dimer microtubules is rather small. These microtubules appear to be stable over a surprisingly wide range of ionic strengths, as also noted by Caplow *et al.* (1989). This may be contrasted with the behaviour of MAP-containing microtubules, which show a distinct ionic strength optimum (Olmsted & Borisy, 1975). This difference is probably related to the effect of ionic strength changes upon MAP-tubulin interactions. Secondly, the effect of changing the ionic strength is the same for changes induced by several different reagents, i.e. for sodium phosphate, NaCl, sodium acetate and Na_2SO_4 . Thirdly, the effect of Mg^{2+} as a promoter of microtubule disassembly is somewhat less pronounced at high concentrations of Pipes (see Fig. 6). Olmsted & Borisy (1975) obtained rather similar results when studying the effect of Na^+ ion on microtubule polymerization for different total concentrations of Pipes.

Effect of solution conditions on microtubule dynamic properties

Dynamic processes in microtubules have, in general, been studied by three methods: (1) observation of the changes in the length distribution of steady-state microtubule populations with time (e.g. see Mitchison & Kirschner, 1984); (2) direct observations of transitions (G-state \rightarrow S-state and S-state \rightarrow G-state) by video microscopy (e.g. Walker *et al.*, 1988) [this method has the advantage of being direct but has the disadvantage that it requires a very large number of observations to obtain reliable averages for state lifetimes (Bayley *et al.*, 1991)]; (3) incorporation of radiolabelled tubulin into a steady-state population of microtubules as used here; inferences of dynamic behaviour are made from the kinetics of the exchange process.

The effects of changes in solution conditions on the kinetics of exchange of tubulin dimer into steady-state microtubules may be briefly summarized as follows. (1) Suppression of microtubule length redistributions at steady state in a glycerol-containing buffer (4.1 M-glycerol plus 10 mM- Mg^{2+}) has been reported by Kristofferson *et al.* (1986). It is also widely known that glycerol greatly lowers the rate of microtubule disassembly induced by extensive dilution (Caplow *et al.*, 1986). We find here that increasing the glycerol concentration suppresses dynamic exchange processes. In the absence of glycerol the value of F_{60} (see above) is 0.62; this is decreased to 0.42 at [glycerol] = 1 M and to less than 0.1 at [glycerol] > 2.5 M. (2) The effect of Ca^{2+} (> 0.1 mM) in accelerating the rate of microtubule dissociation has been known for several years (Karr *et al.*, 1980) and we have shown (Gal *et al.*, 1988) that very similar effects are induced by Mg^{2+} (> 10 mM). More recently, direct observations (O'Brien *et al.*, 1989) have shown that this increase is also seen in the rates of microtubule shortening. These authors also showed that rates of microtubule growth are somewhat enhanced at elevated [Mg^{2+}]. We find here that increasing [Ca^{2+}] or [Mg^{2+}] enhances dynamic exchange processes. For example, the amount of exchange observed in 10 min is more than twice that seen for the control (0.5 mM- Mg^{2+} , no Ca^{2+}) for concentrations of 0.4 mM- and 17 mM- Ca^{2+} and - Mg^{2+} respectively (see Figs. 4a and 5a). (3) The effects of phosphate are controversial. Carlier *et al.* (1989) have reported that microtubules diluted into phosphate-containing buffers disassemble at a greatly decreased rate. However, Caplow *et al.* (1989) have shown that phosphate and sulphate

Table 1. Numerical simulation data

Note (i) For the standard kinetic set, $f_1 = f_2 = 1$; see the text and Bayley *et al.* (1990) for further details. Note (ii) The prime (') attached to \bar{T}_s , \bar{T}_G , R'_s , R'_G and $L'_{av.}$ denotes parameters evaluated at the C_c as shown in column 3.

Rate constants:

$$\begin{aligned}
 k(-D)_{DD} &= f_1 \cdot 200 \text{ s}^{-1} \\
 k(-T)_{DD} &= f_2 \cdot 100 \text{ s}^{-1} \\
 k(-T)_{DT} &= k(-T)_{TD} = f_2 \cdot 10 \text{ s}^{-1} \\
 k(-T)_{TT} &= f_2 \cdot 1 \text{ s}^{-1} \\
 k(+T)_{DD} &= 5 \times 10^5 \text{ M}^{-1} \cdot \text{s}^{-1} \\
 k(+T)_{DT} &= k(+T)_{TD} = k(+T)_{TT} = 2 \times 10^6 \text{ M}^{-1} \cdot \text{s}^{-1}
 \end{aligned}$$

f_1	f_2	C_c (μM)	\bar{T}_s (s)	\bar{T}_G (s)	R'_s ($\mu\text{m}/\text{min}$)	R'_G ($\mu\text{m}/\text{min}$)	$L'_{av.}$ (μm)
Part (a)							
0.50	0.50	5.25	18.4	132.8	-8.4	1.1	2.49
1.00	1.00	10.50	9.9	67.5	-16.1	2.2	2.56
2.00	2.00	21.00	4.3	32.9	-35.5	4.3	2.47
Part (b)							
0.05	1.00	6.65	22.4	18.9	-0.8	0.9	0.32
0.125	1.00	7.60	15.4	24.8	-2.1	1.3	0.53
0.25	1.00	8.40	13.6	32.7	-3.9	1.7	0.86
1.00	1.00	10.50	9.9	67.5	-16.1	2.2	2.56
2.00	1.00	11.80	8.9	128.0	-38.4	2.5	5.58
4.00	1.00	13.25	7.8	216.4	-73.0	2.7	9.65
Part (c)							
0.25	0.50	4.65	19.3	87.8	-4.2	0.9	1.34
1.00	1.00	10.50	9.9	67.5	-16.1	2.2	2.56
3.00	1.50	18.25	5.5	84.2	-54.1	3.8	5.12

have no effect on the rates of microtubule shortening as measured by direct observation by video microscopy. We find here that increasing the ionic strength through the addition of either sodium phosphate or Na_2SO_4 appears to have relatively little effect upon the kinetics of exchange (Fig. 7b).

Kinetic interpretation of changes in microtubule dynamics

A population of microtubules exhibiting dynamic instability consists of two sub-populations, one growing at rate R_G ($= k_{app}^+ \cdot C_c$), and the other shrinking at rate R_S ($= k_{app}^-$), where k_{app}^+ and k_{app}^- are the apparent association and dissociation rate constants (per microtubule end). Interconversions between the growing and shrinking states are characterized by the mean lifetimes of the states (\bar{T}_G and \bar{T}_S). The rate and extent of exchange will depend on the average length of growing and shrinking excursions, $L_{av.(G)}$ ($= R_G \cdot \bar{T}_G$) and $L_{av.(S)}$ ($= R_S \cdot \bar{T}_S$) (at steady state $L'_{av.} = L'_{av.(G)} = L'_{av.(S)} = R'_G \cdot \bar{T}'_G = R'_S \cdot \bar{T}'_S$, with primes denoting values at the C_c) and upon the average length of the microtubule population at the point at which the label is added (Bayley *et al.*, 1989b). Very long microtubules will only be labelled slowly, even though the average excursion length will, of course, be independent of the absolute length. The parameters R'_G , R'_S , C_c , \bar{T}'_S and \bar{T}'_G (which completely define the behaviour of a microtubule population) are all intuitively expected to be determined by the association and dissociation rate constants for Tu-GTP and Tu-GDP at a microtubule end.

In the Lateral Cap formulation for microtubule dynamics, individual rate constants are specified for binding at a site on the microtubule end depending on the nucleotide content (GTP and GDP) of the two adjacent tubulin molecules (xy). There are thus four configurations (xy = TT, TD, DT, DD) defining the constants $k(+T)_{xy}$ and $k(-T)_{xy}$ for association and dissociation of Tu-GTP, and one constant [$k(-D)_{DD}$] for dissociation of Tu-GDP. (Typical values are given in Table 1.) Computer simulation with these rate constants has been shown to generate the characteristic transition properties of dynamic microtubules

(Bayley *et al.*, 1990). Critical concentration is determined as the free [Tu-GTP], which gives zero net growth for an extended simulation; likewise the exchange activity is assessed in terms of $L'_{av.}$, the average excursion length. As this decreases, the extent of exchange clearly decreases (cf. Bayley *et al.*, 1989b).

The question is how might changes in solution composition influence these individual rate constants and hence the C_c and exchange behaviour. It appears (see above) that such changes can have a major effect on the rate of microtubule disassembly, either decreasing it (glycerol) or increasing it (Mg^{2+} or Ca^{2+}). Although all the individual rate constants are probably affected to some extent, we will limit the following discussion to changes in the dissociation rate constants.

Table 1 shows values for various important parameters derived by computer simulation. Part (a) shows the effect of changing all the dissociation rate constants by the same factor ($f_1 = f_2$). Reducing these constants decreases the C_c value (as expected) but has no effect on the efficiency of exchange as measured by the value of $L'_{av.}$. Increasing the dissociation rate constant for loss of Tu-GDP [$k(-D)_{DD}$] increases the shrinking rate R'_S (at the new critical concentration) but shortens the mean lifetime of the shrinking state \bar{T}'_S by a similar factor, so that $L'_{av.(S)}$ ($= R'_S \cdot \bar{T}'_S$) is approximately constant. Part (b) examines the effect of changing $k(-D)_{DD}$ specifically ($f_1 \neq 1, f_2 = 1$), and shows that the extent of exchange ($L'_{av.}$) is markedly sensitive to this parameter, whereas the C_c changes only 2-fold for an 80-fold variation in this constant. This bears out the compensatory effects of changes in these kinetic parameters, noted previously (Bayley *et al.*, 1990). Again it is seen that for $f_1 > 1$ R'_S increases, but \bar{T}'_S decreases less, so that overall $L'_{av.}$ increases. Part (c) shows that increasing all dissociation constants, with a larger increase in $k(-D)_{DD}$ ($f_1 > f_2 > 1$) produces an increased C_c with increased $L'_{av.}$ and hence increased extent of exchange ($f_1 > f_2 > 1$). At the same time, the shrinkage rate R'_S increases more than the growth rate R'_G , and the mean shrinking-state lifetime, \bar{T}'_S , is selectively shortened.

One advantage of studying dynamic effects on microtubule populations is that the system readily adjusts to a new steady state; all the observations of exchange properties in this work are under such conditions. By contrast, experiments with individual microtubules are significantly different. The introduction of an effector (such as Mg^{2+} or Ca^{2+}) inevitably changes the C_c of the macroscopic system, as shown in our experimental results. Observed changes in mean lifetimes of growing and shrinking states of a dynamic microtubule are then difficult to interpret, since such lifetimes are known to be a function of the free Tu-GTP concentration (Walker *et al.*, 1988) and, as we have shown, a function of [Tu-GTP] relative to the new C_c (Bayley *et al.*, 1990). Nonetheless, even the data of Table 1 (which refer throughout to the steady-state condition) show that changes of the dissociation rate constants can produce a number of distinctive dynamic effects. These include (Table 1, part *a*) reciprocal effects in \bar{T}_s and \bar{T}_G with little effect in L'_{av} and large effects in C_c , (Table 1, part *b*) reciprocal effects in \bar{T}_s and \bar{T}_G with pronounced effects in L_{av} and small effects in C_c , and (Table 1, part *c*) differential effects in \bar{T}_s relative to \bar{T}_G with moderate effects in L'_{av} and C_c . Data on the effects of Mg^{2+} and Ca^{2+} on transition behaviour at constant protein concentration have been reported by O'Brien *et al.* (1990*a,b*). These results, though not directly comparable with the calculations of Table 1 for the reasons given, do indicate complex differential effects on mean state lifetimes (and on microtubule polarity). Specifically, the Lateral Cap model shows the contrasting behaviour of G-state and S-state lifetimes as the critical concentration is changed. In a shift of solution conditions at constant protein concentration, C_c , such that $C_{c(new)} > C_{c(old)}$ (as effected by enhanced $[Mg^{2+}]$ or $[Ca^{2+}]$), the change to $C_{c(new)} > C_c$ causes an increase in \bar{T}_s and decrease in \bar{T}_G . This correlates exactly with the data of O'Brien *et al.* (1990*a,b*), where increased $[Mg^{2+}]$ produces an increased \bar{T}_s (lower frequency of rescue, S-state→G-state) and decreased \bar{T}_G (a higher rate of catastrophe, G-state→S-state), at least at microtubule minus ends.

These results show a straightforward correlation of the critical concentration for assembly with dynamic activity of the microtubule population. An increase in C_c (such as generated by increased concentration of Mg^{2+} or added Ca^{2+}) is accompanied by a marked increase in dynamic incorporation of labelled tubulin. And, conversely, a decrease in C_c , as generated by increasing concentrations of glycerol, is accompanied by less dynamic incorporation, and may suppress it altogether at higher concentrations. Whereas changes in the C_c may be the result of changes in a number of kinetic parameters, direct experimental evidence supports an effect of metal ions (or glycerol) in increasing (or decreasing) the dissociation rate constants of the system. In fact, the computer simulation shows that such a change is insufficient to reproduce the additional effects upon the dynamic properties, as assessed by tubulin exchange. A specific change in the dissociation of Tu-GDP relative to the rate constants for the dissociation of Tu-GTP is necessary. Thus, although growth (and assembly) are strictly dependent upon Tu-GTP, a considerable degree of modulation of the dynamic properties is evidently possible through effects of solution components on the rate at which Tu-GDP dissociates during microtubule disassembly.

The reasons for changes in dissociation rate constants with solution conditions are not immediately clear. It is evident that increased [glycerol] enhances tubulin-tubulin interactions, and appears to be responsible for increased lateral interactions between protofilaments, as judged by the generation of tubulin assemblies with aberrant morphology (Karecla *et al.*, 1989). By contrast, elevated $[Mg^{2+}]$ promotes the formation of oligomeric species from Tu-GDP (Howard & Timasheff, 1986), which

would be consistent with the enhancement by Mg^{2+} of longitudinal interactions in the direction of the protofilament axis. Both of these effects, having their basis in tubulin-tubulin interactions, but with different spatial properties, could account for the observed changes in kinetics. These actions appear to be relatively low-affinity, and hence rather unspecific. This lack of specificity may be contrasted with the highly specific high-affinity substoichiometric effects of various anti-mitotic drugs such as podophyllotoxin and colchicine in causing a selective reduction in microtubule dynamics *in vitro* (Schilstra *et al.*, 1989; A. Vancandelaere, M. J. Schilstra, P. M. Bayley, Y. Engelborghs & S. R. Martin, unpublished work). These effects imply specific interactions with terminal sites in the microtubule, which are seen in numerical simulations based on the Lateral Cap principle to be able dramatically to reduce microtubule length excursions (Bayley *et al.*, 1991). Thus regulation of microtubule dynamics can be effected through intrinsic kinetic properties by agents acting at different levels of concentration and hence selectivity. Both specific and unspecific modulation of dynamics can be rationalized in terms of effects on a limited number of kinetic parameters in the Lateral Cap formulation of microtubule dynamic instability.

This work was supported in part under E.E.C. Twinning Grant no. 852/00255/UK/05PUJU1.

REFERENCES

- Bayley, P. M. (1990) *J. Cell Sci.* **95**, 329–334
 Bayley, P. M. & Martin, S. R. (1989) *Biophys. J.* **55**, 256a
 Bayley, P. M., Butler, F. M. M., Clark, D. C., Manser, E. J. & Martin, S. R. (1985) *Biochem. J.* **227**, 439–455
 Bayley, P. M., Schilstra, M. J. & Martin, S. R. (1988) *Biophys. J.* **53**, 29a
 Bayley, P. M., Schilstra, M. J. & Martin, S. R. (1989*a*) *FEBS Lett.* **259**, 181–184
 Bayley, P. M., Schilstra, M. J. & Martin, S. R. (1989*b*) *J. Cell Sci.* **93**, 241–254
 Bayley, P. M., Gal, V., Karecla, P., Martin, S. R., Schilstra, M. J. & Engelborghs, Y. (1989*c*) *Springer Ser. Biophys.* **3**, 249–258
 Bayley, P. M., Schilstra, M. J. & Martin, S. R. (1990) *J. Cell Sci.* **95**, 33–48
 Bayley, P. M., Martin, S. R., Sharma, K. K. (1991) in *The Living Cell in its Four Dimensions* (Trojanowski, C., ed.), American Institute of Physics, Washington, in the press
 Bevington, P. R. (1969) *Data Reduction and Error Analysis for the Physical Sciences*, pp. 236–236, McGraw-Hill, New York
 Caplow, M., Shanks, J. & Brylawski, B. P. (1986) *J. Biol. Chem.* **261**, 16233–16240
 Caplow, M., Ruhlen, R., Shanks, J., Walker, R. A. & Salmon, E. D. (1989) *Biochemistry* **28**, 8136–8141
 Carlier, M. F. & Pantaloni, D. (1981) *Biochemistry* **20**, 1918–1924
 Carlier, M. F., Didry, D. & Pantaloni, D. (1987) *Biochemistry* **26**, 4428–4437
 Carlier, M. F., Didry, D., Melki, R., Chabre, M. & Pantaloni, D. (1988) *Biochemistry* **27**, 3555–3559
 Carlier, M., Didry, D., Simon, C. & Pantaloni, D. (1989) *Biochemistry* **28**, 1783–1791
 Cassimeris, L. U., Pryer, N. K. & Salmon, E. D. (1988) *J. Cell Biol.* **107**, 2223–2231
 Chen, Y. & Hill, T. L. (1985*a*) *Proc. Natl. Acad. Sci. U.S.A.* **82**, 1131–1135
 Chen, Y. & Hill, T. L. (1985*b*) *Proc. Natl. Acad. Sci. U.S.A.* **82**, 4127–4131
 Clark, D. C., Martin, S. R. & Bayley, P. M. (1981) *Biochemistry* **20**, 1924–1932
 Engelborghs, Y. (1989) in *Microtubule Proteins* (Avila, J., ed.), pp. 1–36, CRC Press, Boca Raton
 Gal, V., Martin, S. R. & Bayley, P. M. (1988) *Biochem. Biophys. Res. Commun.* **155**, 1464–1470
 Hill, T. L. (1984) *Proc. Natl. Acad. Sci. U.S.A.* **81**, 6728–6732
 Horio, T. & Hotani, H. (1986) *Nature (London)* **321**, 605–607
 Howard, W. D. & Timasheff, S. N. (1986) *Biochemistry* **25**, 8292–8300

- Karecla, P., Hirst, E. & Bayley, P. (1989) *J. Cell Sci.* **94**, 479–488
- Karr, T. L., Kristofferson, D. & Purich, D. L. (1980) *J. Biol. Chem.* **255**, 11853–11856
- Keates, R. A. B. (1980) *Biochem. Biophys. Res. Commun.* **97**, 1163–1169
- Keates, R. A. B. (1981) *Can. J. Biochem.* **59**, 353–360
- Kirschner, M. W. (1989) *Harvey Lect.* **83**, 1–20
- Kirschner, M. W. & Mitchison, T. (1986) *Cell* **45**, 329–342
- Kristofferson, D., Mitchison, T. & Kirschner, M. W. (1986) *J. Cell Biol.* **102**, 1007–1019
- Martin, S. R., Butler, F. M. M., Clark, D. C., Zhou, J.-M. & Bayley, P. M. (1987a) *Biochim. Biophys. Acta* **914**, 96–100
- Martin, S. R., Schilstra, M. J. & Bayley, P. M. (1987b) *Biochem. Biophys. Res. Commun.* **149**, 461–467
- Martin, S. R., Schilstra, M. J. & Bayley, P. M. (1991) *Biochim. Biophys. Acta* **1073**, 551–561
- Mitchison, T. & Kirschner, M. W. (1984) *Nature (London)* **312**, 237–242
- O'Brien, E. T., Voter, W. A. & Erickson, H. P. (1987) *Biochemistry* **26**, 4148–4156
- O'Brien, E. T., Walker, R. A., Salmon, E. D. & Erickson, H. P. (1989) *Springer Ser. Biophys.* **3**, 259–261
- O'Brien, E. T., Erickson, H. P. & Salmon, E. D. (1990a) *J. Cell Biol.* **111**, 388a
- O'Brien, E. T., Salmon, E. D., Walker, R. A. & Erickson, H. P. (1990b) *Biochemistry* **29**, 6648–6656
- Olmsted, J. B. & Borisy, G. G. (1975) *Biochemistry* **14**, 2996–3005
- Parness, J. & Horwitz, S. B. (1981) *J. Cell Biol.* **91**, 479–487
- Sammak, P. J. & Borisy, G. G. (1988) *Nature (London)* **332**, 724–726
- Schilstra, M. J., Martin, S. R. & Bayley, P. M. (1987) *Biochem. Biophys. Res. Commun.* **147**, 588–595
- Schilstra, M. J., Martin, S. R. & Bayley, P. M. (1988) *Inst. Natl. Sante Rech. Med. Colloq.* **171**, 43–49
- Schilstra, M. J., Martin, S. R. & Bayley, P. M. (1989) *J. Biol. Chem.* **264**, 8827–8834
- Schulze, E. & Kirschner, M. W. (1988) *Nature (London)* **334**, 356–359
- Stewart, R. J., Farrell, K. W. & Wilson, L. (1990) *Biochemistry* **29**, 6489–6498
- Voter, W. A., O'Brien, E. T. & Erickson, H. P. (1987) *Biophys. J.* **51**, 214a
- Walker, R. A., O'Brien, E. T., Pryer, N. K., Soboeiro, M. F., Voter, W. A. & Erickson, H. P. (1988) *J. Cell Biol.* **107**, 1437–1488
- Wani, M. C., Taylor, H. L., Wall, M. E., Coggon, P. & McPhail, A. T. (1971) *J. Am. Chem. Soc.* **93**, 2325–2327
- Wilson, L., Miller, H. P. & Farrell, K. W. (1990) *J. Cell Biol.* **111**, 28a

Received 17 January 1991; accepted 21 February 1991